



RESEARCH ARTICLE

Fenofibrate Inhibits Hepatic Stellate Cell Activation and Autophagy in Liver Fibrosis through the TGFβ1/Smad3 and PPARα/cGAS/STING Pathways

Ziqi Cheng^{1,5#}, Liu Fu², Malire Yimamu¹, Jiao Feng¹, Liwei Wu³, Yunzhao Hu⁴, Jianye Wu², Xuanfu Xu^{6**} and Chuanyong Guo^{1*}

¹Department of Gastroenterology, Shanghai Tenth People's Hospital, Tongji University School of Medicine, Shanghai 200072, China; ²Department of Gastroenterology, Putuo People's Hospital, Tongji University School of Medicine, Shanghai 200060, China; ³Department of Gastroenterology, Shanghai East Hospital, Tongji University School of Medicine, Shanghai 200120, China; ⁴Department of Laboratory Medicine, Shanghai Traditional Chinese Medicine-Integrated Hospital, Shanghai University of Traditional Chinese Medicine, Shanghai, China; ⁵Laboratory Animal Center, Shanghai Tenth People's Hospital, Tongji University School of Medicine, Shanghai 200072, China; ⁶Department of Gastroenterology, Shidong Hospital, Shanghai 200433, China.# Author makes the main contribution to this work.

*Corresponding author: shuanfusky@163.com (Xuanfu Xu); guochuanyong@hotmail.com (Chuanyong Guo)

ARTICLE HISTORY (25-206)

Received: March 8, 2025
Revised: April 22, 2025
Accepted: April 24, 2025
Published online: May 05, 2025

Key words:

Autophagy
Fenofibrate
Liver fibrosis
Ppara/cgas/sting
Tgfβ1/smad3

ABSTRACT

Liver fibrosis is a typical feature of abnormal liver structure and excessive collagen deposition. It is a chronic liver disease with some potential for reversal. Nonetheless, liver fibrosis remains a formidable clinical challenge. In this study, we investigated the anti-fibrotic mechanisms of fenofibrate and its therapeutic potential in liver fibrosis. Two liver fibrosis models were established in C57BL/6 mice: one induced by intraperitoneal carbon tetrachloride (CCl₄) administration for 8 weeks, and the other by bile duct ligation (BDL) for 2 weeks. The BDL procedure involved exposing the common bile duct, followed by ligation and transection between the two tied points. Fenofibrate (50 and 100mg/kg) was administered via intraperitoneal injection three times per week. Gene and protein expression levels in tissues and cells were analyzed using RT-qPCR, Western blot, immunohistochemistry (IHC), immunofluorescence (IF), and other relevant techniques. Liver tissues were utilized for histological staining and transmission electron microscopy (TEM). The results showed that fenofibrate did not induce significant toxicity to the liver. Fenofibrate alleviated extracellular matrix (ECM) deposition in BDL and CCl₄-mediated liver fibrosis models and regulated the balance between tissue inhibitor of metalloproteinase (TIMP)-2 and matrix metalloproteinase (MMP)-2. Fenofibrate reduced hepatic stellate cells (HSCs) activation and autophagy through the peroxisome proliferator-activated receptor alpha (PPARα)/cyclic GMP-AMP synthase (cGAS)/stimulator of interferon genes (STING) and transforming growth factor beta 1 (TGFβ1)/smad family member 3 (smad3) pathways. To summarize, fenofibrate alleviated liver fibrosis through suppressing HSCs activation.

To Cite This Article: Cheng Z, Fu L, Yimamu M, Feng J, Wu L, Hu Y, Wu J, Xu X and Guo C, 2025. Fenofibrate Inhibits Hepatic Stellate Cell Activation and Autophagy in Liver Fibrosis through the Tgfβ1/Smad3 and Ppara/Cgas/Sting Pathways. Pak Vet J. <http://dx.doi.org/10.29261/pakvetj/2025.161>

INTRODUCTION

Chronic liver damage over an extended period can result in liver cirrhosis, fibrosis, or liver cancer (Abou Monsef and Kutsal, 2021; Acharya *et al.*, 2021; Savić *et al.*, 2024). Although previously considered a prolonged and irreversible process, some research has suggested that this progression is not entirely uncontrollable (Ramachandran *et al.*, 2015; Pearson and Thomson, 2024). By removing risk factors and applying active treatment, the remarkable

regenerative capacity of the liver can reverse such damage (Martello *et al.*, 2023; Feng *et al.*, 2024). However, if a persistent wound-healing response occurs, it promotes hepatic stellate cell (HSC) activation, which then causes HSCs to transform into myofibroblasts from the quiescent state (Dou *et al.*, 2018; Krenkel *et al.*, 2019)

HSCs can be detected primarily in the sub endothelial space of Disse within the liver (Chauhan *et al.*, 2024). Abnormal HSCs activity disrupts the extracellular matrix (ECM) and excessive synthesis or insufficient degradation

of the ECM can lead to scarce replacement of the normal liver structure (Gupta *et al.*, 2019). No effective anti-fibrotic drugs are available for controlling the progression of fibrosis (Shan *et al.*, 2022). Therefore, elucidating the molecular mechanisms and potential therapeutic targets of liver fibrosis is extremely important for improving disease outcomes.

Autophagy is a process that involves intracellular waste degradation and recycling and exerts an important effect on maintaining intracellular homeostasis and organelle renewal (Ferrara *et al.*, 2023). This process involves basal autophagy and autophagy induced by stress (Sun *et al.*, 2021). The former serves as a protective mechanism and promotes cell growth (Kar *et al.*, 2019). However, an overabundance of autophagy might induce metabolic stress, disrupt cellular components, and even lead to cell death (Slavin *et al.*, 2018). Autophagy manifests differently in different cells. In HSCs, abnormal autophagy promotes their activation, enhances the synthesis and secretion of the ECM, and provides the energy necessary for ECM production (Kim *et al.*, 2017).

The ECM provides structural support to cells, modulates cell activity, and provides important biological information for the proper functioning of the body (Strackeljan *et al.*, 2021). The ECM can continuously activate HSCs via relevant signaling pathways. Notably, the TGF- β /Smad pathway is crucial for liver fibrosis. TGF- β 1 is an important driver of HSC activation and binds to its receptors T β RI and T β RII. Downstream Smad2/3 is activated and translocated to the nucleus. Thus, it exerts a key effect on modulating fibrosis-related gene levels (Denton *et al.*, 2005; Kim *et al.*, 2020). TGF- β /Smad pathway enhances autophagy within cells associated with fibrosis by increasing autophagy-related gene levels, such as Bcl-2-Interacting Protein (Beclin)-1 and Microtubule-Associated Protein 1 Light Chain (LC3)-II (Ding *et al.*, 2014).

Abnormal DNA in the cytoplasm activates cGAS and later produces 2'3' cyclic GMP-AMP (cGAMP), a second messenger. This cGAMP can combine with STING and activate it, further activating TBK1 and inducing the nuclear transport of IRF3 and NF- κ B (two transcription factors) (Yum *et al.*, 2021; Balka *et al.*, 2023; Pan *et al.*, 2023). cGAS/STING pathway activation is tightly associated with cell autophagy. Beclin-1 phosphorylates TBK1 (Yamano *et al.*, 2024), and STING partially colocalizes with LC3 (Gui *et al.*, 2019; Liu *et al.*, 2019). This mechanism indicates that the pathway is upstream of autophagy, where it senses damaged DNA and stress signals, triggers autophagy, and facilitates cellular clearance.

Fenofibrate is a drug that is used for treating cardiovascular disease and hyperlipidemia (Miceli *et al.*, 2021; Munro *et al.*, 2021). Mostly, it is used to treat hyperlipidemia, diabetes, and atherosclerosis in humans, but its effects have also been studied in animals (Crakes *et al.*, 2021). It is a peroxisome proliferator-activated receptor α (PPAR α) agonist. PPAR α , a nuclear receptor, inhibits liver fibrosis development through modulating lipid metabolism, suppressing inflammatory responses, while alleviating oxidative stress (Chen *et al.*, 2021; Echeverria-Villalobos *et al.*, 2024). It can inhibit the TGF- β /Smad pathway and reduce signal transmission.

PPAR α significantly inhibits cGAS and STING, thus alleviating inflammation and the formation of new blood vessels (Lyu *et al.*, 2024). These findings indicate that fenofibrate can modulate both pathways to achieve anti-fibrotic effects.

This study assessed how fenofibrate affects the TGF- β /Smad and cGAS/STING signaling pathways in two animal models: CCl₄ and bile duct ligation (BDL). We found that fenofibrate ameliorated liver fibrogenesis by suppressing HSC activation and modulating autophagy through these two pathways. These findings provided information on the associations of these genes with autophagy and new targets for treating fibrosis.

MATERIALS AND METHODS

Reagents: Fenofibrate was purchased from MedChemExpress (Shanghai, China). Pentobarbital sodium salt was provided by Sigma-Aldrich Co. (St. Louis, MO, USA), while carbon tetrachloride (CCl₄) was obtained in China Sinopharm International Corporation (Shanghai, China). Kits used to analyze alanine aspartate aminotransferase (AST), aminotransferase (ALT), and hydroxyproline levels were acquired in the Jiancheng Bioengineering Institute in Nanjing, China. Primary antibodies against Beclin-1, LC3, p62, MMP2, TIMP2, α -SMA, PPAR α , cGAS, and STING were provided by Proteintech (Chicago, IL, USA). Collagen I, TGF- β 1, Smad3, and p-Smad3 antibodies were acquired in Abcam (Cambridge, MA, USA). The PCR kit was obtained in Takara (Takara Biotechnology, Dalian, China).

Animals: Shanghai SLAC Laboratory Animal Co., Ltd. provided eight-week-old male C57BL/6 mice (body weight: 23 \pm 3g) for this study. The mice were maintained under standard conditions (24 \pm 2°C and 60% humidity) and were allowed to drink water and take food freely. Animal experiments followed guidelines provided by National Institutes of Health (NIH) and gained approval from the Animal Care and Use Committee of Tongji University, Shanghai.

Model establishment and drug treatment

Preliminary experiment: In total, we randomized 20 mice in four groups (n=5 each). The control group was not treated, while the vehicle group was given intraperitoneal injections of peanut oil thrice weekly for two weeks. The FF group was intraperitoneally injected with 100mg/kg fenofibrate thrice weekly for two weeks. Mice in the sham group underwent sham surgery. Fenofibrate was blended sufficiently with corn oil, and two weeks later, the animals were euthanized through cervical dislocation. Then, serum and liver samples were harvested for ALT and AST measurements and pathological analysis.

Main experiments: For the BDL-mediated liver fibrosis model, the C57BL/6 mice were starved for a 24h period prior to anesthesia by intraperitoneal injection with 1.25% sodium pentobarbital (Nembutal, St. Louis, MO, USA). After opening the abdominal cavity, a portion of the bile duct was exposed, ligated at both ends, and severed between the ligatures, and finally, the abdominal cavity was closed. Following BDL surgery, fenofibrate was

administered intraperitoneally, starting on the second day. Next, we randomized 24 animals as four groups (n=6 each): 1) Sham group: animals undergoing laparotomy with no BDL; 2) BDL group: animals undergoing the BDL operation; 3) fenofibrate 50mg/kg group: BDL animals that were administered 50mg/kg fenofibrate thrice weekly for two weeks; 4) fenofibrate 100mg/kg group: BDL animals that were administered 100mg/kg fenofibrate thrice every week for two weeks. Blood and liver samples were harvested in subsequent analyses.

For the liver fibrosis model induced by CCl₄, the animals were given an injection of 10% CCl₄ (1.0mL/kg, dissolved in peanut oil) thrice weekly for eight weeks. Fenofibrate (50 or 100mg/kg) was administered intraperitoneally during this period. A total of 24 animals were divided as four groups (n=6): 1) Vehicle group given intraperitoneal injection of peanut oil; 2) CCl₄ group given CCl₄ injection; 3) fenofibrate 50mg/kg; mice were administered both CCl₄ and 50mg/kg fenofibrate thrice every week for two weeks; 4) fenofibrate 100mg/kg; mice were administered CCl₄ and 100mg/kg fenofibrate thrice every week for two weeks. Blood and liver specimens were harvested in subsequent assays.

Cell culture and CCK8 assay: We cultivated human immortal LX2 cells within high-glucose DMEM that contained 10% FBS as well as 1% penicillin-streptomycin. Cells of logarithmic growth phase were subsequently inoculated in 96-well plates prior to 48h of culture and an additional 24h of 0–48μM FF treatment. The 96-well plate was placed in a microplate reader, and the optical density (OD) was measured at a wavelength of 450nm to calculate cell viability.

Biochemical assays: Blood was sampled and preserved at -80°C, followed by 10min of centrifugation at 4600×g to separate the serum, which was subsequently preserved under -80°C. AST and ALT levels were detected using the automatic chemical analyzer (Olympus AU1000, Olympus, Tokyo, Japan). Hydroxyproline content was measured using a corresponding kit following specific protocols.

Histopathology: Liver left lobe samples were fixed within 4% formaldehyde before gradient ethanol dehydration, paraffin embedding, and preparation into 5μm tissue sections for hematoxylin and eosin (H&E) staining for assessing liver damage. Collagen deposition was detected using Masson's trichrome (MT) staining. The MT staining procedure involved sequentially adding modified Weigert's iron hematoxylin, Biebrich scarlet-acid fuchsin solution, and aniline blue for staining.

Quantitative real-time reverse transcription-polymerase chain reaction (qRT-PCR): This study utilized the TRIzol reagent (Tiangen Biotech, Beijing, China) for extracting total RNA following specific protocols, which was then used for preparing cDNA via reverse-transcription. The specific experimental procedures were as follows: After lysing the samples with TRIzol, chloroform was added for shaking and extraction. The supernatant was then collected and precipitated with isopropanol. The precipitate was subsequently dissolved in

RNase-free water to measure the RNA concentration. We then utilized the 7900HT Fast Real-Time PCR system (Applied Biosystems, Foster City, CA, USA) (Wawrusiewicz-Kurylonek *et al.*, 2020), SYBR Green qRT-PCR for measuring gene expression (Çelik *et al.*, 2023). All primers adopted in PCR can be observed from Table 1.

Table 1: Primer sequences in qRT-PCR

| Gene | Primer (5'-3') | |
|----------|----------------|-------------------------|
| Col-1 | Forward | CAATGGCACGGCTGTGTGCG |
| | Reverse | AGCACTCGCCCTCCCCTCTT |
| α-SMA | Forward | CCCAGACATCAGGGAGTAATGG |
| | Reverse | TCTATCGGATACTTCAGCGTCA |
| Beclin-1 | Forward | ATGGAGGGGTCTAAGCGCTC |
| | Reverse | TGGGCTGTGGTAAGTAATGGA |
| LC3 | Forward | GACCGCTGTAAAGAGGTGC |
| | Reverse | AGAAGCCGAAGTTTCTTGGG |
| p62 | Forward | GAGCACCCCCGAAACATGG |
| | Reverse | ACTTATAGCGAGTTCCCACCA |
| TIMP1 | Forward | CGAGACCACCTTATACCAGCG |
| | Reverse | ATGACTGGGGTGTAGGCGTA |
| MMP2 | Forward | GGACAAGTGGTCCGCGTAAA |
| | Reverse | CCGACCGTTGAACAGGAAGG |
| TGF-β1 | Forward | CCACCTGCAAGACCATCGAC |
| | Reverse | CTGGCGAGCCTTAGTTTGGAC |
| PPARα | Forward | ACCACTACGGAGTTTACGCATG |
| | Reverse | GAATCTTGCAGCTCCGATCACAC |
| cGAS | Forward | TTCCACGAGGAAATCCGCTGAG |
| | Reverse | CAGCAGGGCTTCTGGTTTTTC |
| STING | Forward | CACGCGTCCGCCAC |
| | Reverse | TCGAGACTCGGGACATCTT |
| β-actin | Forward | GGCTGTATTCCCCTCCATCG |
| | Reverse | CCAGTTGGTAACAATGCCATGT |

Western blot: We adopted RIPA lysis buffer for extracting total protein, after which we used the BCA kit for measuring the protein content. The proteins were preserved at -20°C. Then, protein aliquots (80μg) were used to perform 7.5–12.5% SDS-PAGE for separation, after which they were added into polyvinylidene difluoride (PVDF) or nitrocellulose (NC) membranes. After 1h of blocking with 5% defatted milk for preventing nonspecific binding, primary antibodies were added to incubate membranes overnight under 4°C. After 10min of washing by PBS that contained 0.05% Tween-20 (PBST) three times, membranes were further probed using secondary antibodies under ambient temperature for a 1h duration. After rinsing with PBST for 30min, samples were evaluated using the Odyssey Infrared Imaging System (LI-COR Biosciences, Lincoln, NE, USA).

Immunohistochemical staining: After the liver tissue sections were embedded in paraffin, they underwent deparaffinization and rehydration. The sections were heated for a 1h duration within citrate buffer (pH 6.0) under 60°C for antigen retrieval, later treated with 3% hydrogen peroxide for blocking endogenous peroxidase activity, whereas 5% bovine serum albumin (BSA) was added to block nonspecific binding sites. Primary antibodies (1:500 dilution) were subsequently added to incubate membranes overnight under 4°C. Later, secondary antibodies matching the host species of the primary antibodies were utilized to incubate samples under ambient temperature for a 30min duration. An optical microscope was used to observe the samples, and the integral optical density (IOD) was determined using the Image-Pro Plus software 6.0 (Media Cybernetics, Silver Spring, MD, USA).

Immunofluorescence staining: Following cell plating, the coverslips were removed and rinsed with PBS, followed by fixation with 4% paraformaldehyde and 5% BSA blocking. We later incubated coverslips overnight using primary antibodies (1:500 dilution in 3% BSA) under 4°C. Following PBS rinsing, secondary antibodies labeled through fluorescence matching the host species of the primary antibodies were applied for a 1h duration at ambient temperature. Following PBS washing, DAPI was adopted for nuclear visualization. A mounting medium containing the anti-fluorescence quenching agent was used, and the fluorescence microscope was applied in capturing fluorescence images.

Transmission electron microscopy: The 3% glutaraldehyde was added to fix liver samples, followed by epoxy resin embedding and cutting into thin slices (1.5µm thick) for staining with toluidine blue. Ultrastructure was monitored under the transmission electron microscope (JEM 1230; JEOL, Tokyo, Japan).

Statistical analysis: This study utilized GraphPad Prism version 10.0 for making figures and performing statistical analysis. The results were analyzed with Student's t test and one-way ANOVA analysis. Data were represented by mean ± standard deviation (SD). P<0.05 stood for statistical significance.

RESULTS

Fenofibrate does not cause significant toxicity to the liver structure or function: To exclude the potential effects of surgery or the drug alone on liver function, we compared groups treated with a sham operation, vehicle, FF, and the control. ALT and AST levels in blood serum were analyzed, while the hydroxyproline content was

assessed in liver tissue. No significant liver damage was found among the different groups (Fig. 1A-C). H&E staining revealed no adverse effects on liver structure (Fig. 1 D), indicating that neither surgery nor drug treatment induced noticeable liver damage.

Fenofibrate alleviates CCl₄-induced and BDL-induced liver fibrosis: To evaluate whether fenofibrate positively affects liver function in fibrosis models, we measured ALT, AST, and hydroxyproline levels in the plasma and liver tissue (Fig. 2A-C). Compared to the control group, CCl₄ and BDL groups presented markedly greater ALT, AST, and hydroxyproline contents. However, the intraperitoneal injection of fenofibrate substantially decreased liver damage. A CCK8 assay was also conducted to determine the IC₅₀ of FF in cell experiments, which was found to be 27.08µM (Fig. 2D). Therefore, concentrations of 24µM (L) and 30µM (H) were selected for further cell experiments. Liver tissue staining (Fig. 2E) revealed that in the vehicle and sham groups, the cytoplasm was clear with prominent nuclei and nucleoli. The BDL group exhibited cholangiolar hyperplasia, collagen deposition in the portal area, and liver tissue structural reorganization. The CCl₄ group exhibited hepatocyte swelling, vacuolization, necrosis, inflammation, and abnormal collagen fiber proliferation. After treatment with fenofibrate, these liver abnormalities were significantly reduced. MT staining of liver tissue showed a similar pattern of collagen deposition. Thus, fenofibrate has beneficial effects on fibrosis.

Fenofibrate inhibits ECM production: The Col-1 and α-SMA contents remarkably increased in model groups compared with the control group (Fig. 3A). These results matched the Western blot and qRT-PCR results (Fig. 3B-D). After treatment with FF, these changes were reversed in a dose-dependent manner. COL1 also significantly

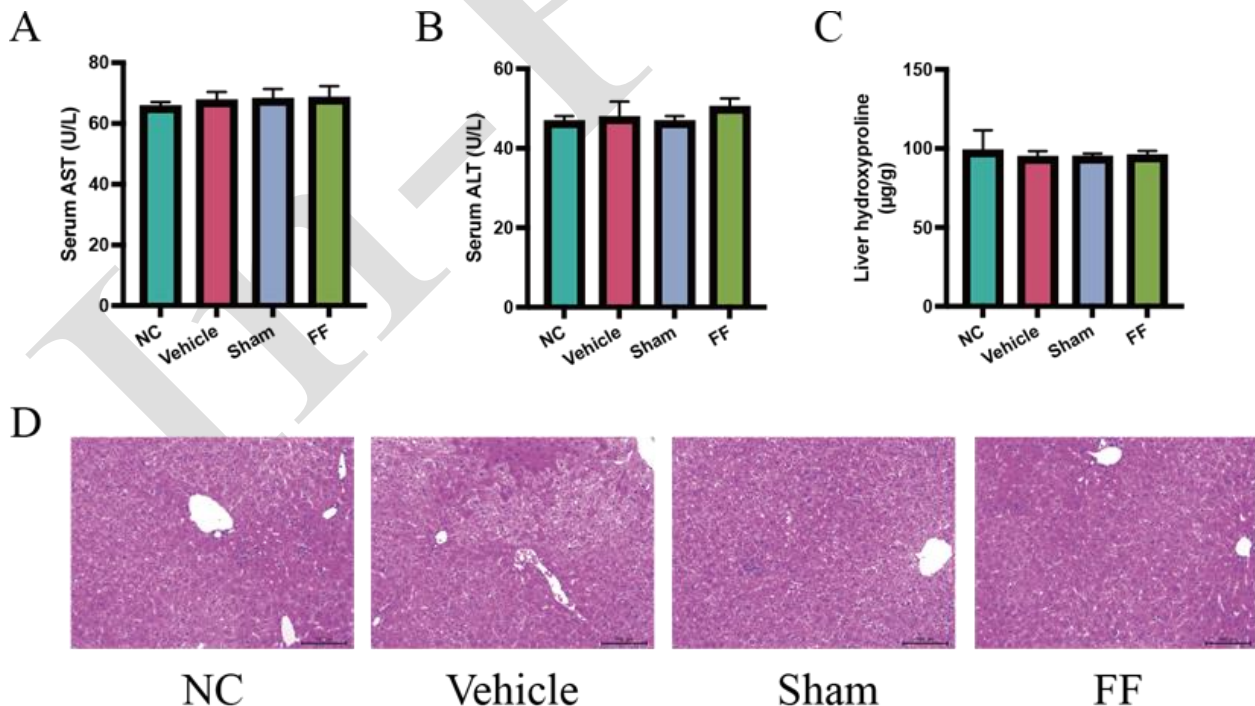


Fig. 1: Effects of fenofibrate administration and surgery on normal mice. (A-C) Serum ALT, AST, and liver hydroxyproline levels of the four groups were not significantly different. Data are represented by mean ± SD (n=5, P>0.05). (D) Typical H&E-stained liver sections (original magnification, ×200).

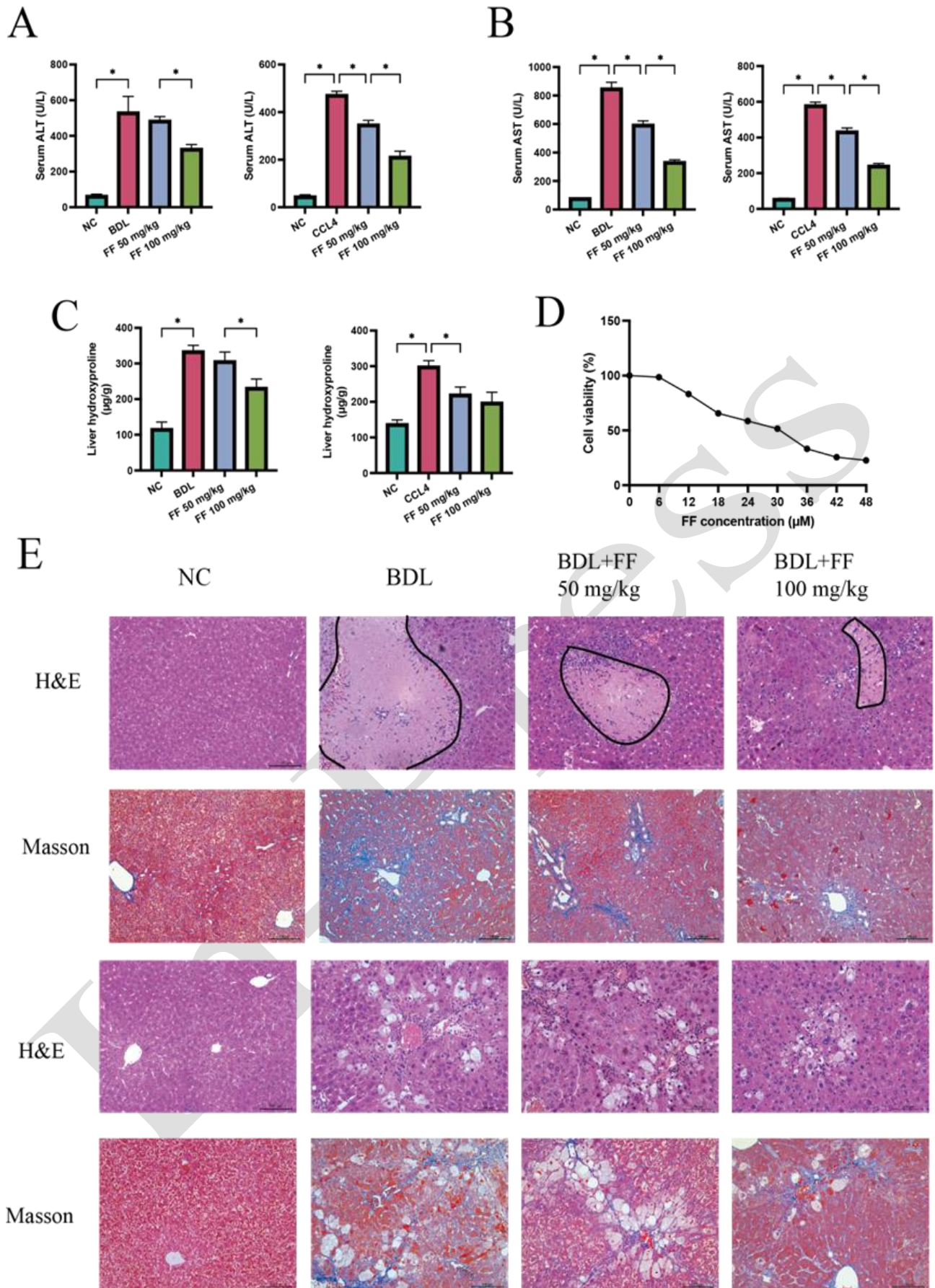


Fig. 2: Roles of FF in liver function and pathology in BDL-induced and CCL₄-mediated liver fibrosis. (A) Serum ALT contents represented by mean \pm SD (n=6; *P<0.05). (B) Serum AST contents represented by mean \pm SD (n=6; *P<0.05). (C) Hydroxyproline contents represented by mean \pm SD (n=6; *P<0.05). (D) Cytotoxicity induced by different concentrations of FF in LX2 cells analyzed through CCK8 assay. (E) Effects of FF on pathological changes during liver fibrosis were visualized through H&E and Masson's trichrome staining (original magnification, \times 200).

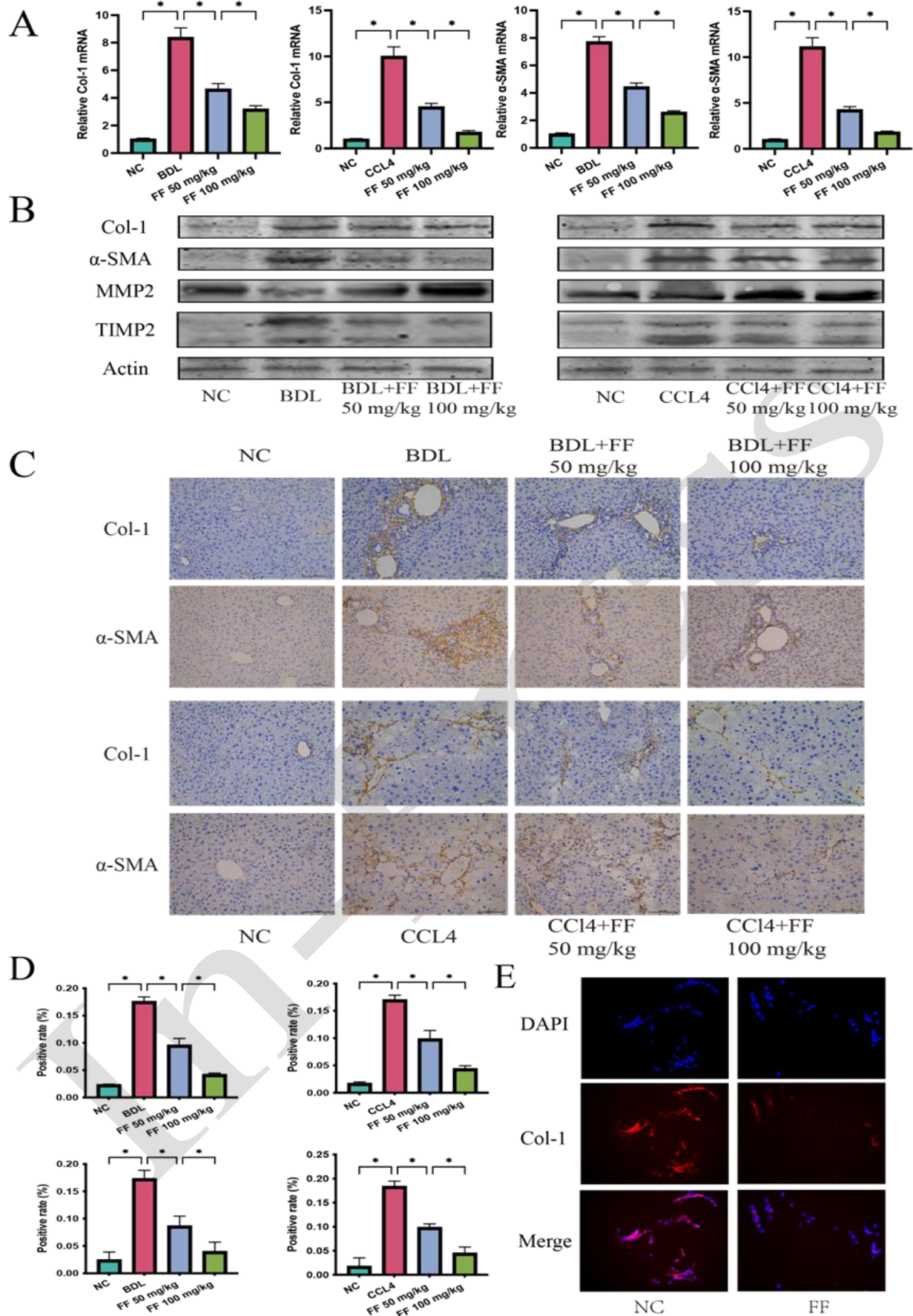


Fig. 3: FF regulated the activation of HSCs and balanced TIMP1 and MMP2. (A) Relative Col-I and α -SMA levels determined through qRT-PCR and represented by the mean \pm SD ($n=3$; $*P<0.05$). (B) Western blot conducted for measuring Col-I, α -SMA, TIMP2, and MMP2 protein levels. (C & D) Col-I and α -SMA protein expression within liver tissues was evaluated through immunohistochemistry. The positively stained area proportion was determined by the Image-Pro Plus 6.0 software (original magnification, $\times 200$; $n=3$; $*P<0.05$). (E) Immunofluorescence (IF) staining of Col-I within LX2 cells from NC and FF(H) groups (original magnification, $\times 200$).

changed in LX2 cells (Fig. 3E). Protein analysis of mouse tissues revealed that MMP-2 was up-regulated, whereas TIMP-2 was down-regulated in the fenofibrate groups (Fig. 3B). These results suggested that fenofibrate inhibits ECM production and regulates the MMP/TIMP balance in liver fibrosis.

Fenofibrate inhibits autophagic activity in liver fibrosis: For determining how autophagy affected liver fibrosis, this study assessed Beclin-1, sequestosome 1 (p62), and LC3 (autophagy markers) levels by conducting qRT-PCR assays (Fig. 4A). Beclin-1 was found to promote autophagosome formation, and LC3 expression considerably increased in model groups, whereas p62 expression was lower. Fenofibrate treatment reversed these changes in a dose-dependent manner. Transmission electron microscopy (TEM) revealed more autophagosomes in the BDL and CCl₄ groups than in the other groups (Fig. 4B). The results of the Western blot and immunohistochemistry assays confirmed these findings (Fig. 4C-D). Additionally, when an autophagy activator, the soybean peptide QRPR, was applied to LX2 cells, the antifibrotic effect of fenofibrate was inhibited (Fig. 4E). To summarize, fenofibrate alleviates the autophagic activity associated with liver fibrosis.

Fenofibrate inhibits HSC activation via the TGFβ1/Smad3 and PPARα/cGAS/STING pathways: We examined cGAS and STING RNA levels and found that their expression was upregulated under conditions of fibrosis (Fig. 5A). After treatment with fenofibrate, the expression levels decreased. TGFβ1/Smad3 is a classic fibrogenic pathway. By measuring TGF-β1 protein levels, we found that fenofibrate mitigated the harmful effects of BDL and CCl₄ on the liver (Fig. 5B-C). The level of protein expression in animals and cells was consistent with these results (Fig. 5D). After drug treatment, PPARα was regulated, while TGF-β1 expression was downregulated. TGF-β1 activates the receptor and phosphorylates Smad3, inducing ECM synthesis and deposition and promoting the activation and trans-differentiation of HSCs. Based on qRT-PCR, Western blot, and immunohistochemistry assays, Smad3 levels did not change significantly in the model group, but p-Smad3 levels were upregulated. This change was reversed by fenofibrate, with consistent results observed in cells.

DISCUSSION

Liver fibrosis, the frequently reported pathological process, results from different factors, with a common reason being chronic liver injury (Bao *et al.*, 2021; Saravanan and Ramkumar, 2024; Ling *et al.*, 2025). Fenofibrate mainly regulates lipid metabolism through activating PPARα; it displays strong anti-inflammatory (Nakanishi *et al.*, 2023) and antioxidant activities (Ibáñez *et al.*, 2023). Researchers have primarily investigated its effects on hyperlipidemia (Miceli *et al.*, 2022), diabetes (Alsaleem *et al.*, 2025), and atherosclerosis (Spartalis *et al.*, 2021) in humans and animals. However, the role of fenofibrate in liver fibrosis remains unclear.

The safety profile of the drug significantly influences its progression from the laboratory research to the clinical

application. No significant differences in liver injury were found among the sham operation, vehicle, FF, and control groups. This result indicated that fenofibrate is not toxic to the liver, conforming to prior findings of applying fenofibrate in treating metabolic diseases.

Fenofibrate showed significant protective effects on liver fibrosis models caused by CCl₄ and BDL, alleviating liver injury and related symptoms of fibrosis. Fenofibrate exerts therapeutic effects by lowering ALT and AST levels, reducing hepatocellular damage, and mitigating structural changes in the liver. The CCl₄ and BDL models are important experimental models for research on liver fibrosis; the CCl₄ model is widely used to simulate toxin-induced liver injury (Zira *et al.*, 2013), and the BDL model induces liver injury and fibrosis through biliary obstruction (Tag *et al.*, 2015). The use of both models increases the reliability of the results and broadens the applicability of the study. Antifibrotic drugs mainly focus on small molecules or TGF-β signaling inhibitors (Nanthakumar *et al.*, 2015; Luangmonkong *et al.*, 2018; Vistnes, 2024), but there are no effective drugs that specifically target liver fibrosis, especially those that can reverse established fibrosis. Fenofibrate may reveal a new strategy to treat liver fibrosis.

Based on the results of the preliminary experiment, we initially concluded that fenofibrate had no significant toxic or side effects in mice. Consequently, we proceeded to conduct the formal experiment on mice. During fibrosis, the accumulation of ECM, particularly collagen (COL1) deposition, is a hallmark of liver fibrosis (Parsons *et al.*, 2007), and an increase in ECM deposition is closely associated with activated HSCs expressing α-smooth muscle actin (α-SMA) (Kato *et al.*, 2020). Activated fibroblasts promote collagen synthesis through the expression of α-SMA, which is tightly associated with fibrosis occurrence. The normal ECM composition is generally balanced, but in fibrosis, excessive ECM synthesis coupled with restricted degradation leads to structural changes and impaired liver function (Matsuda and Seki, 2020). The results of this study suggested that fenofibrate, by downregulating COL1 and α-SMA expression, may help restore the ECM balance and delay or reverse liver fibrosis. ECM degradation can be modulated by matrix metalloproteinases (MMPs), whose activity is controlled by TIMPs (Bourbouli and Stetler-Stevenson, 2010). MMP2 is a key enzyme in COL1 degradation, and TIMP-2 is its primary inhibitor (Li *et al.*, 2018). We found that after fenofibrate treatment, MMP-2 activity increased while TIMP-2 levels decreased, indicating that fenofibrate promoted ECM degradation by modulating the MMP/TIMP balance, further decreasing the progression of fibrosis. This action was also reported in humans and animals (Shan *et al.*, 2023), suggesting that regulation of the MMP/TIMP balance can effectively control ECM metabolism and prevent the progression of fibrosis.

Autophagy is activated in cells under stress (such as nutrient deprivation, oxidative stress, and injury) for organelle degradation and material recycling. HSCs activation accounts for the core process during liver fibrosis and requires substantial energy and metabolic resources for cell proliferation, migration, and ECM synthesis. Autophagy helps provide these metabolic resources by degrading intracellular components to produce fatty acids, amino acids, and nucleotides (Durrant *et al.*, 2016; Ma *et al.*, 2018).

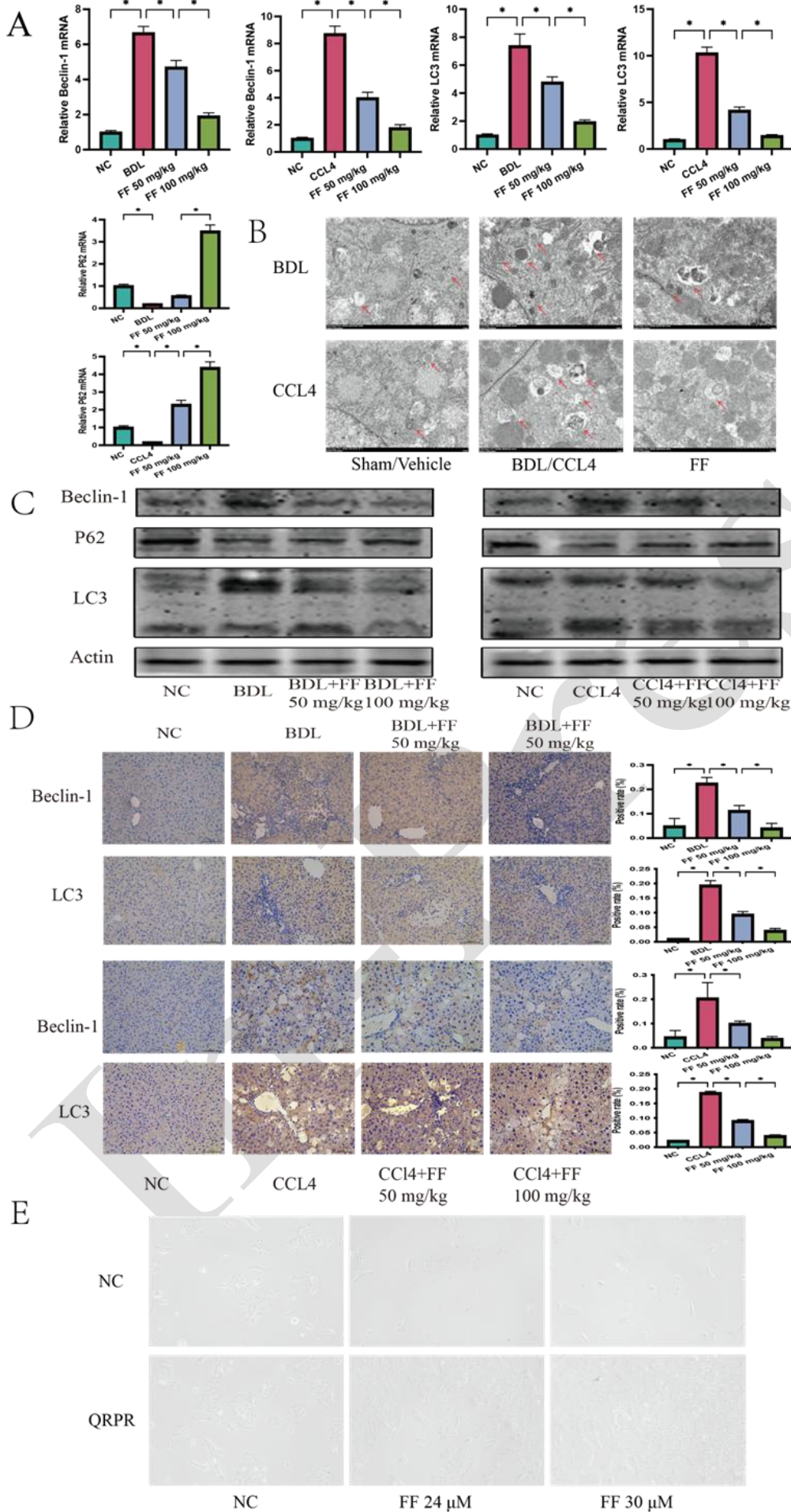
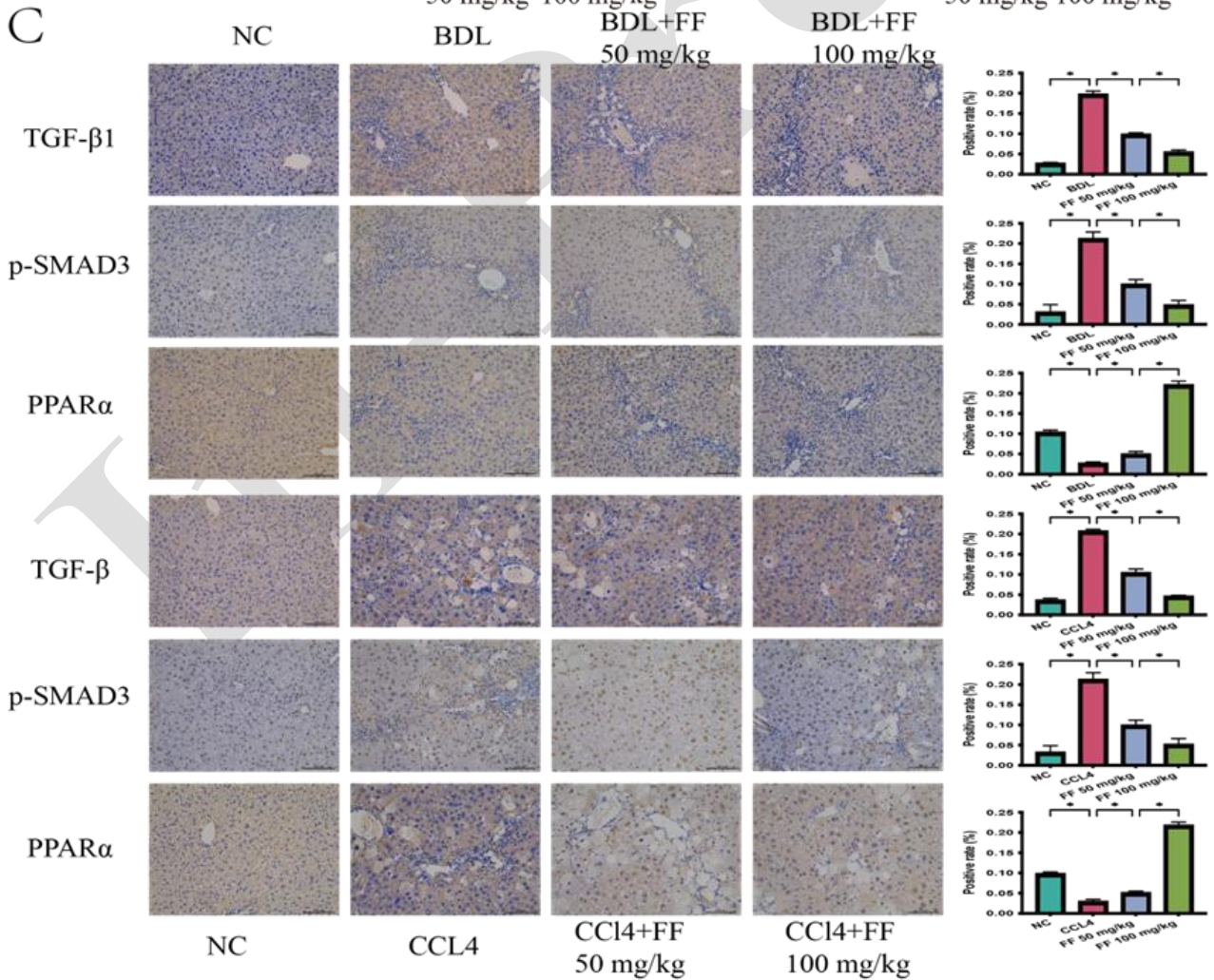
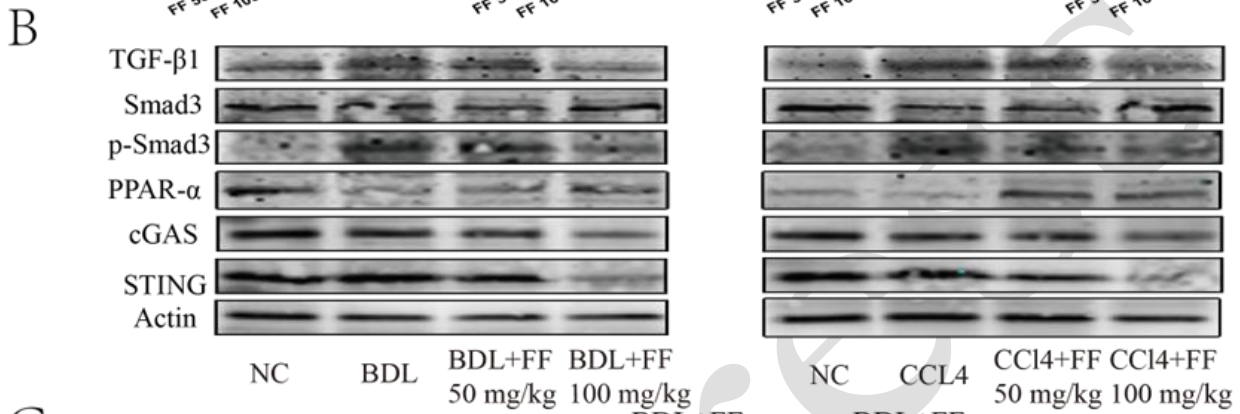
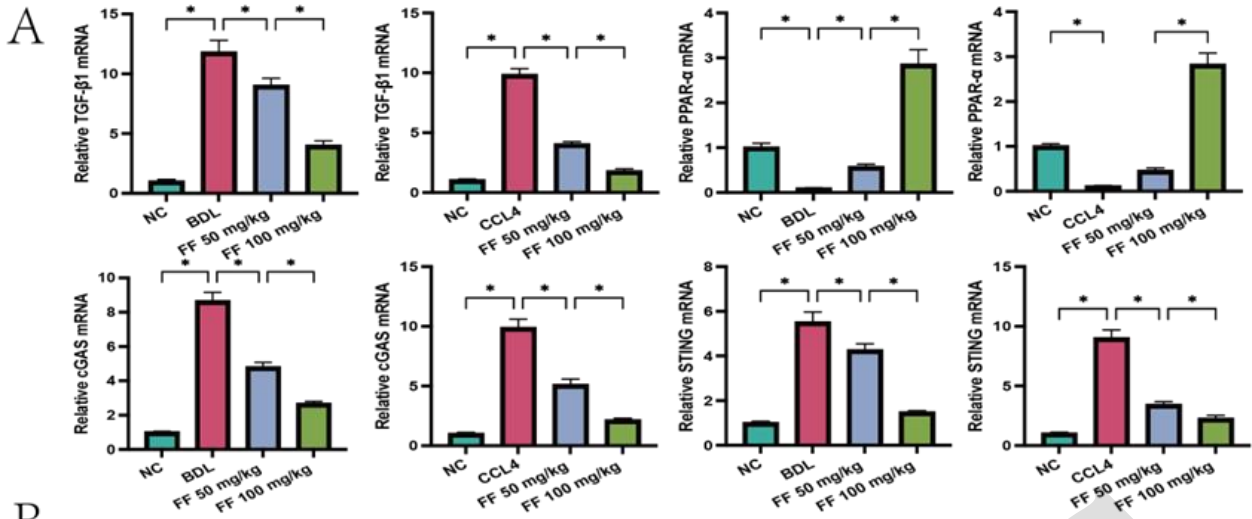


Fig. 4: The effect of FF on autophagy. (A) The relative levels of Beclin-1, LC3, and P62 were determined through qRT-PCR and represented by mean \pm SD (n=3; *P<0.05). (B) TEM analysis of autophagosome formation in the Sham/Vehicle, BDL/CCL4, and FF(H) groups (red arrows). (C) Western blot conducted for measuring Beclin-1, LC3, and P62 protein levels. (D) Beclin-1 and LC3 protein levels within liver tissues were detected through immunohistochemical analysis. The positively stained area proportion determined by the Image-Pro Plus 6.0 software (original magnification, \times 200; n=3; *P<0.05). (E) Cell growth was observed in the presence of the autophagy inhibitor soybean peptide QRPR under a microscope (original magnification, \times 200).



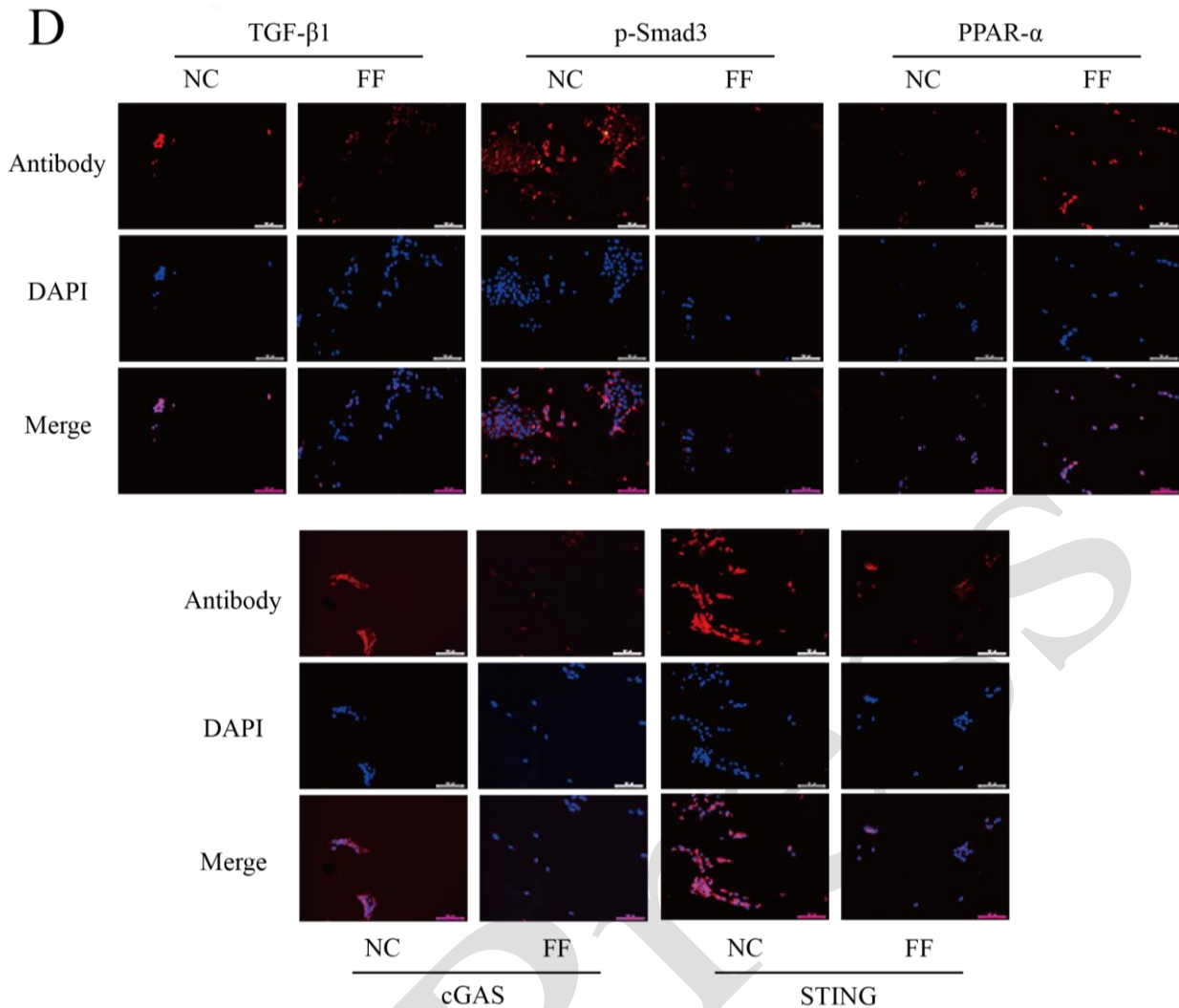


Fig. 5: FF alleviated liver fibrosis through the TGF- β 1/Smad3 and cGAS/STING pathways. (A) TGF- β 1, PPAR α , cGAS, and STING levels were measured through qRT-PCR and represented by mean \pm SD (n=3; *P<0.05). (B) Western blot conducted for determining TGF- β 1, Smad3, p-Smad3, PPAR α , cGAS, and STING protein levels. (C) Immunohistochemical staining was performed to evaluate TGF- β 1, p-Smad3, and PPAR α protein levels within liver tissues. The positively stained area proportion determined by the Image-Pro Plus 6.0 software (original magnification, \times 200; n=3; *P<0.05). (D) IF staining was performed to detect TGF- β 1, p-Smad3, PPAR α , cGAS, and STING within LX2 cells from NC and FF(H) groups (original magnification, \times 200).

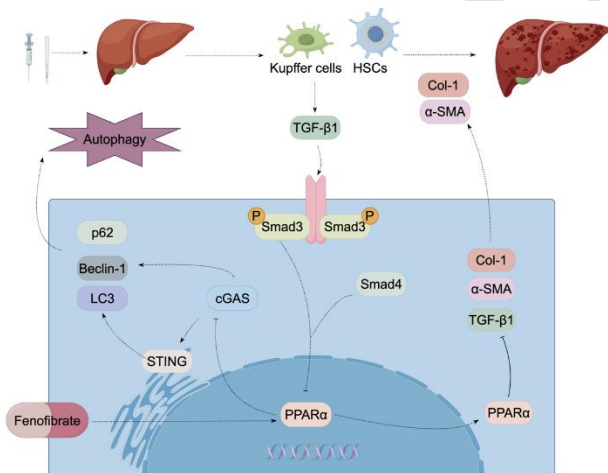


Fig. 6: The potential mechanism of the efficacy of FF in liver fibrosis. Note: Fenofibrate inhibits liver fibrosis by TGF- β 1/Smad3 and PPAR α /cGAS/STING pathways. After TGF- β 1 binds to the receptor, smad3 is activated to generate the complex with Smad4, and it then enters nucleus to exert its effects. Moreover, PPAR α inhibits TGF- β 1 and cGAS; cGAS acts on STING and Beclin-1, and STING acts on LC3. When fenofibrate activates PPAR α , this anti-autophagic effect is enhanced, thereby exerting an anti-liver fibrosis effect.

By improving autophagosome formation and autophagy markers Beclin-1 and LC3 levels, fenofibrate may inhibit the excessive activation of HSCs, thus alleviating collagen accumulation and the development of liver fibrosis (Fan *et al.*, 2024; Liu *et al.*, 2024). Beclin-1 and LC3 are key autophagy markers; Beclin-1 promotes autophagosome formation (Quiles *et al.*, 2023), and LC3 is a component of the autophagosomal membrane (Kabeya *et al.*, 2000). The autophagy receptor p62 binds and labels substances for degradation (Liu *et al.*, 2016). A decrease in p62 levels generally indicates insufficient clearance of degraded substances, which may lead to the accumulation of toxic materials (Wang *et al.*, 2019). In this study, a recovery experiment was conducted for verifying the inhibition of fenofibrate against autophagy of liver fibrosis.

PPAR α has an important effect on resisting liver fibrosis through modulating inflammatory responses and fatty acid metabolism (Devchand *et al.*, 1996). In fibrosis, PPAR α inhibits TGF- β 1/Smad-3 pathway activation, reducing the activation and transdifferentiation of fibroblasts (Lyu *et al.*, 2019). Fenofibrate can reverse TGF- β 1 up-regulation and down-regulate p-Smad3 levels,

supporting PPAR α 's ability to modulate the TGF- β 1/Smad-3 pathway.

cGAS/STING pathway accounts for a DNA-sensing pathway closely related to autophagy. After DNA is stimulated, STING interacts with the autophagy marker LC3, and cGAS interacts with Beclin-1 to promote autophagy (Liang *et al.*, 2014). The cGAS/STING pathway has aroused great interest recently; studies have suggested its involvement in liver fibrosis, although the exact mechanism remains unclear (Chen *et al.*, 2022; Liang *et al.*, 2022). TGF- β 1 can also regulate the activity of PPAR α , affecting cellular lipid metabolism and renal fibrosis (Sekiguchi *et al.*, 2007; Lyu *et al.*, 2019). A similar study conducted by Crakes *et al.* (2021) concluded that administration of fenofibrate in canines regulates the PPAR α , thus reducing the triacylglycerol, diacylglycerol in blood and prevents liver damage. The cGAS and STING levels increased within liver fibrosis models and decreased after treatment with fenofibrate. These findings suggested that fenofibrate may regulate autophagy by suppressing cGAS/STING pathway, thus affecting HSCs activation and liver fibrosis development. Research showed that after the knockout of the PPAR α gene, cGAS and STING are significantly upregulated. PPAR α mediates the cGAS/STING pathway, regulates mitochondrial function, and influences cell activation (Dong *et al.*, 2023; Pan *et al.*, 2025). The relationship of cGAS/STING pathway with autophagy involves interaction between STING and the autophagy marker LC3. After DNA damage, the association between cGAS and Beclin-1 further promotes autophagy, and this may protect against fibrosis by removing damaged cells and limiting fibrosis occurrence. TGF- β 1 activation promotes ECM deposition, whereas the STING pathway is related to regulating the degree of deposition by modulating autophagic responses (Fig. 6).

Although this study provided important information on the application of fenofibrate in the treatment of liver fibrosis, it has several limitations. First, the animal models used (such as BDL and CCl₄ treatment) are common, but they may not fully mimic the complex mechanisms of human liver fibrosis, especially in the context of fibrosis induced by different etiologies, where differences between models may limit clinical applicability. Second, the short-term experiments did not fully reflect whether fenofibrate is safe and effective in the long term to treat chronic diseases (Cho and Park, 2014; Wrońska *et al.*, 2024; Kobuchi *et al.*, 2025). While experiments have shown that fenofibrate can inhibit ECM production, its efficacy in different fibrosis models and clinical safety needs further verification. Lastly, the study focused on specific pathways; other mechanisms by which fenofibrate may be exerting its effects could be explored.

To summarize, we speculated that fenofibrate can significantly alleviate the progression of fibrosis. Fenofibrate reduced ECM accumulation and alleviated excessive autophagy in liver fibrosis through TGF- β 1/Smad-3 and PPAR α /cGAS/STING pathways.

Data availability: Data utilized for supporting our results are available from corresponding author on request.

Conflicts of interest: All authors disclosed no relevant relationships.

Funding: This work was supported by the National Natural Science Foundation of China (Grant No. 82300655), the Health System Innovation Project of Shanghai Putuo Science and Technology Commission (Grant No. PTKWWS202303), Traditional Chinese Medicine Scientific Research Project of Shanghai Hongkou District Health Commission in 2023 (Grant No. HKQGYQ-ZYY-2023-18) and China Postdoctoral Science Foundation (Grant No. 2022M712412, 2023M732655).

Authors Contribution: Ziqi Cheng: Writing – original draft, Visualization, Validation, Investigation. Liu Fu: Writing – original draft, Methodology, Formal analysis. Malire Yimamu: Software, Investigation, Data curation. Jiao Feng: Funding acquisition, Validation, Methodology. Liwei Wu: Funding acquisition, Software, Resources. Yunzhao Hu: Investigation, Methodology, Funding acquisition. Jianye Wu: Funding acquisition, Data curation. Xuanfu Xu: Writing – review & editing, Supervision, Conceptualization. Chuanyong Guo: Writing – review & editing, Project administration, Funding acquisition.

Acknowledgements: Figdraw (www.figdraw.com) was used for picture materials (ID: ASPPP50121).

REFERENCES

- Abou Monsef Y and Kutsal O, 2021. Pathomorphological evaluation of hepatobiliary lesions in dogs and cats of Ankara region/Patomorfološka procjena hepatobilijarnih lezija u pasa i macaka uzgojenih na području grada Ankare. *Vet Arh* 91(4):359-379.
- Acharya P, Chouhan K, Weiskirchen S, *et al.*, 2021. Cellular mechanisms of liver fibrosis. *Front Pharmacol* 12:671640.
- Alsalem MA, Al-Kuraishy HM, Al-Gareeb AI, *et al.*, 2025. Decrypting the possible mechanistic role of fenofibrate in alzheimer's disease and type 2 diabetes: The truth and mystery. *J Cell Mol Med* 29(5):e70378.
- Balka KR, Venkatraman R, Saunders TL, *et al.*, 2023. Termination of STING responses is mediated via ESCRT-dependent degradation. *EMBO J* 42(12): e112712.
- Bao YL, Wang L, Pan HT, *et al.*, 2021. Animal and organoid models of liver fibrosis. *Front Physiol* 12:666138.
- Bourboullia D and Stetler-Stevenson WG, 2010). Matrix metalloproteinases (MMPs) and tissue inhibitors of metalloproteinases (TIMPs): Positive and negative regulators in tumor cell adhesion. In: *Seminars in Cancer Biology*. Academic Press. 22(3):161-168.
- Çelik A, Emiralioglu O, Yeken MZ, *et al.*, 2023. A novel study on bean common mosaic virus accumulation shows disease resistance at the initial stage of infection in *Phaseolus vulgaris*. *Front Genet* 14:1136794.
- Chauhan RS, Malik YS, Saminathan M, *et al.*, 2024. Immunopathology of the Liver in Animals. In: *Essentials of Veterinary Immunology and Immunopathology Singapore*: Springer Nature, Singapore. pp.217-252.
- Chen L, Xia S, Wang S, *et al.*, 2022. Naringenin is a potential immunomodulator for inhibiting liver fibrosis by inhibiting the cGAS-STING pathway. *J Clin Transl Hepatol* 11(1):26.
- Chen X, He W, Sun M, *et al.*, 2021. STING inhibition accelerates the bone healing process while enhancing type H vessel formation. *Fed Am Soc Exp Biol* 35(11): e21964.
- Cho YD and Park YJ, 2014. In vitro and in vivo evaluation of a self-microemulsifying drug delivery system for the poorly soluble drug fenofibrate. *Arch Pharmacol Res* 37(2):193-203.
- Crakes KR, Pires J, Quach N, *et al.*, 2021. Fenofibrate promotes PPAR α -targeted recovery of the intestinal epithelial barrier at the host-microbe interface in dogs with diabetes mellitus. *Sci Rep* 11(1):13454.

- Denton CP, Lindahl GE, Khan K, et al., 2005. Activation of key profibrotic mechanisms in transgenic fibroblasts expressing kinase-deficient type II transforming growth factor- β receptor (TBR116k). *J Biol Chem* 280(16):16053-16065.
- Devchand PR, Keller H, Peters JM, et al., 1996. The PPAR α -leukotriene B4 pathway to inflammation control. *Nature* 384(6604):39-43.
- Ding Y, Il Kim S, Lee SY, et al., 2014. Autophagy regulates TGF- β expression and suppresses kidney fibrosis induced by unilateral ureteral obstruction. *J Am Soc Nephrol* 25(12):2835-2846.
- Dong L, Cheng R, Ma X, et al., 2023. Regulation of monocyte activation by PPAR α through interaction with the cGAS-STING pathway. *Diabetes* 72(7):958-972.
- Dou C, Liu Z, Tu K, et al., 2018. P300 acetyltransferase mediates stiffness-induced activation of hepatic stellate cells into tumor-promoting myofibroblasts. *Gastroenterology* 154(8):2209-2221.
- Durrant LG, Metheringham RL and Brentville VA, 2016. Autophagy, citrullination and cancer. *Autophagy* 12(6):1055-1056.
- Echeverria-Villalobos M, Guevara Y, Mitchell J, et al., 2024. Potential perioperative cardiovascular outcomes in cannabis/cannabinoid users. A call for caution. *Front Cardiovasc Med* 11:1343549.
- Fan S, Gao Y, Zhao P, et al., 2024. Fenofibrate-promoted hepatomegaly and liver regeneration are PPAR α -dependent and partially related to the YAP pathway. *Acta Pharm Sin B* 14(7):2992-3008.
- Feng G, Valenti L, Wong VWS, et al., 2024. Re-compensation in cirrhosis: Unravelling the evolving natural history of nonalcoholic fatty liver disease. *Nat Rev Gastroenterol Hepatol* 21(1):46-56.
- Ferrara G, Sgadari M, Longobardi C, et al., 2023. Autophagy up-regulation upon FeHV-1 infection on permissive cells. *Front Vet Sci* 10:1174681.
- Gui X, Yang H, Li T, et al., 2019. Autophagy induction via STING trafficking is a primordial function of the cGAS pathway. *Nature* 567(7747):262-266.
- Gupta G, Khadem F, and Uzonna JE, 2019. Role of hepatic stellate cell (HSC)-derived cytokines in hepatic inflammation and immunity. *Cytokine* 124:154542.
- Ibáñez C, Acuña T, Quintanilla ME, et al., 2023. Fenofibrate decreases ethanol-induced neuroinflammation and oxidative stress and reduces alcohol relapse in rats by a PPAR- α -dependent mechanism. *Antioxidants* 12(9):1758.
- Kabaya Y, Mizushima N, Ueno T, et al., 2000. LC3, a mammalian homologue of yeast Apg8p, is localized in autophagosomal membranes after processing. *EMBO J* 19(21):5720.
- Kar R, Riquelme MA, Hua R, et al., 2019. Glucocorticoid-induced autophagy protects osteocytes against oxidative stress through activation of MAPK/ERK Signaling. *JBMR Plus* 3(4):e10077.
- Katoh D, Kozuka Y, Noro A, et al., 2020. Tenascin-C induces phenotypic changes in fibroblasts to myofibroblasts with high contractility through the integrin α v β 11/transforming growth factor β /SMAD signaling axis in human breast cancer. *Am J Pathol* 190:2123-2135.
- Kim J, Kang W, Kang SH, et al., 2020. Proline-rich tyrosine kinase 2 mediates transforming growth factor-beta-induced hepatic stellate cell activation and liver fibrosis. *Sci Rep* 10(1):21018.
- Kim KM, Han CY, Kim JY, et al., 2018. G α 12 overexpression induced by miR-16 dysregulation contributes to liver fibrosis by promoting autophagy in hepatic stellate cells. *J Hepatol* 68(3):493-504.
- Kobuchi S, Sugiyama D, Ima A, et al., 2025. Data mining of the FDA adverse event reporting system and animal experiments for assessment of rhabdomyolysis risk associated with lipid-lowering drugs. *Int J Med Sci* 22(7):1485.
- Krenkel O, Hundertmark J, Ritz TP, et al., 2019. Single cell RNA sequencing identifies subsets of hepatic stellate cells and myofibroblasts in liver fibrosis. *Cells* 8(5):503.
- Li CX, Cui LH, Zhuo YZ, et al., 2018. Inhibiting autophagy promotes collagen degradation by regulating matrix metalloproteinases in pancreatic stellate cells. *Life Sciences* 208:276-283.
- Liang L, Shen Y, Hu Y, et al., 2022. cGAS exacerbates *Schistosoma japonicum* infection in a STING-type I IFN-dependent and independent manner. *PLoS Pathog* 18(2):e1010233.
- Liang Q, Seo GJ, Choi YJ, et al., 2014. Crosstalk between the cGAS DNA sensor and Beclin-1 autophagy protein shapes innate antimicrobial immune responses. *Cell Host Microbe* 15(2):228-238.
- Ling L, Li R, Xu M, et al., 2025. Species differences of fatty liver diseases: Comparisons between human and feline. *Amer J Physiol Endocrinol Metab* 328(1):E46-E61.
- Liu C, Li S, Zhang C, et al., 2024. Recent advances in research on active compounds against hepatic fibrosis. *Curr Med Chem* 31(18):2571-2628.
- Liu D, Wu H, Wang C, et al., 2019. STING directly activates autophagy to tune the innate immune response. *Cell Death Differ* 26(9):1735-1749.
- Liu WJ, Ye L, Huang WF, et al., 2016. p62 links the autophagy pathway and the ubiquitin-proteasome system upon ubiquitinated protein degradation. *Cell Mol Biol Lett* 21:1-14.
- Luangmonkong T, Suriguga S, Adhyatmika A, et al., 2018. In vitro and ex vivo anti-fibrotic effects of LY2109761, a small molecule inhibitor against TGF- β . *Toxicol Appl Pharmacol* 355:127-137.
- Lyu H, Li X, Wu Q, et al., 2019. Overexpression of microRNA-21 mediates Ang II-induced renal fibrosis by activating the TGF- β /Smad3 pathway via suppressing PPAR α . *J Pharmacol Sci* 141(1):70-78.
- Lyu S, Zhang T, Peng P, et al., 2024. Involvement of cGAS/STING signaling in the pathogenesis of *Candida albicans* keratitis: insights from genetic and pharmacological approaches. *Investig Ophthalmol Vis Sci* 65(6):13-13.
- Ma Y, Zhou Y, Zhu YC, et al., 2018. Lipophagy contributes to testosterone biosynthesis in male rat Leydig cells. *Endocrinology* 159(2):1119-1129.
- Martello E, Perondi F, Bisanzio D, et al., 2023. Antioxidant effect of a dietary supplement containing fermentative S-acetyl-glutathione and silybin in dogs with liver disease. *Vet Sci* 10(2):131.
- Matsuda M and Seki E, 2020. The liver fibrosis niche: Novel insights into the interplay between fibrosis-composing mesenchymal cells, immune cells, endothelial cells, and extracellular matrix. *Food Chem Toxicol* 143:111556.
- Miceli DD, Guevara JM, Ferraris S, et al., 2022. Therapy for feline secondary hypertriglyceridemia with fenofibrate. *J Feline Med Surg* 24(8):e251-e257.
- Miceli DD, Vidal VP, Blatter MFC, et al., 2021. Fenofibrate treatment for severe hypertriglyceridemia in dogs. *Domest Anim Endocrinol* 74:106578.
- Munro MJ, Hulsebosch SE, Marks SL, et al., 2021. Efficacy of a micronized, nanocrystal fenofibrate formulation in treatment of hyperlipidemia in dogs. *J Vet Intern Med* 35(4):1733-1742.
- Nakanishi T, Izumi M, Suzuki R, et al., 2023. In vitro characterization of anti-inflammatory activities of 3RS, 7R, 11R-phytanic acid. *J Dairy Res* 90(1):92-99.
- Nanthakumar CB, Hatley RJ, Lemma S, et al., 2015. Dissecting fibrosis: therapeutic insights from the small-molecule toolbox. *Nat Rev Drug Discov* 14(10):693-720.
- Pan B, Zhang Z, Ye D, et al., 2025. PPAR α suppresses growth of hepatocellular carcinoma in a high-fat diet context by reducing neutrophil extracellular trap release. *JHEP Reports* 7(1):101228.
- Pan J, Fei CJ, Hu Y, et al., 2023. Current understanding of the cGAS-STING signaling pathway: Structure, regulatory mechanisms, and related diseases. *Zool Res* 44(1):183.
- Parsons CJ, Takashima M and Rippe RA, 2007. Molecular mechanisms of hepatic fibrogenesis. *J Gastroenterol Hepatol* 22:S79-S84.
- Pearson J and Thomson E, 2024. Decompensated liver cirrhosis. *Anaesth Intensive Care Med* 25(1):42-47.
- Quiles J, Najor R, Gonzalez E, et al., 2023. Deciphering functional roles and interplay between Beclin1 and Beclin2 in autophagosome formation and mitophagy. *Science Signaling* 16.
- Ramachandran P, Iredale JP and Fallowfield JA, 2015. Resolution of liver fibrosis: basic mechanisms and clinical relevance. In: *Seminars in liver disease*. Thieme Medical Publishers. 35(2):119-131.
- Saravanan M and Ramkumar PK, 2024. Diseases of hepatobiliary system of dogs and cats. In: *Introduction to Diseases, Diagnosis, and Management of Dogs and Cats*. Academic Press. pp.377-393.
- Savić B, Milovanović B, Stanojević S, et al., 2024. Congenital hepatic fibrosis in an aborted Holstein-Friesian fetus. *Acta Vet Beograd* 74(2):313-321.
- Sekiguchi K, Tian Q, Ishiyama M, et al., 2007. Inhibition of PPAR- α activity in mice with cardiac-restricted expression of tumor necrosis factor: potential role of TGF- β /Smad3. *Am J Physiol Heart Circ Physiol* 292(3): H1443-H1451.
- Shan L, Wang F, Zhai D, et al., 2022. New drugs for hepatic fibrosis. *Front Pharmacol* 13:874408.
- Shan L, Wang F, Zhai D, et al., 2023. Matrix metalloproteinases induce extracellular matrix degradation through various pathways to alleviate hepatic fibrosis. *Biomed Pharmacother* 161:114472.
- Slavin SA, Leonard A, Grose V, et al., 2018. Autophagy inhibitor 3-methyladenine protects against endothelial cell barrier dysfunction in acute lung injury. *American J Physiol Lung Cell Mol Physiol* 314(3):L388-L396.

- Spartalis M, Siasos G, Mastrogeorgiou M, *et al.*, 2021. The effect of per os colchicine administration in combination with fenofibrate and N-acetylcysteine on triglyceride levels and the development of atherosclerotic lesions in cholesterol-fed rabbits. *Eur Rev Med Pharmacol Sci* 25(24).
- Strackeljan L, Baczynska E, Cangalaya C, *et al.*, 2021. Microglia depletion-induced remodeling of extracellular matrix and excitatory synapses in the hippocampus of adult mice. *Cells* 10(8):1862.
- Sun X, Chang R, Tang Y, *et al.*, 2021. Transcription factor EB (TFEB)-mediated autophagy protects bovine mammary epithelial cells against H₂O₂-induced oxidative damage in vitro. *J Anim Sci Biotechnol* 12:1-11.
- Tag CG, Weiskirchen S, Hittatiya K, *et al.*, 2015. Induction of experimental obstructive cholestasis in mice. *Lab Anim* 49:70-80.
- Vistnes, M., 2024. Hitting the Target! Challenges and Opportunities for TGF- β Inhibition for the Treatment of Cardiac fibrosis. *Pharmaceuticals* 17.
- Wang L, Howell ME, Sparks-Wallace A, *et al.*, 2019. p62-mediated Selective autophagy endows virus-transformed cells with insusceptibility to DNA damage under oxidative stress. *PLoS Pathog* 15(4):e1007541.
- Wawrusiewicz-Kurylonek N, Krętownski AJ & Posmyk R, 2020. Frequency of thrombophilia associated genes variants: population-based study. *BMC Med Genet* 21(1): 198.
- Yamano K, Sawada M, Kikuchi R, *et al.*, 2024. Optineurin provides a mitophagy contact site for TBK1 activation. *EMBO J* 43(5):754-779.
- Yum S, Li M, Fang Y, *et al.*, 2021. TBK1 recruitment to STING activates both IRF3 and NF- κ B that mediate immune defense against tumors and viral infections. *Proc Natl Acad Sci* 118(14): e2100225118.
- Zira A, Kostidis S, Theocharis S, *et al.*, 2013. 1H NMR-based metabonomics approach in a rat model of acute liver injury and regeneration induced by CCl₄ administration. *Toxicology* 303:115-124.

EB-Press